

# We are IntechOpen, the world's leading publisher of Open Access books Built by scientists, for scientists

4,800

Open access books available

122,000

International authors and editors

135M

Downloads

Our authors are among the

154

Countries delivered to

TOP 1%

most cited scientists

12.2%

Contributors from top 500 universities



WEB OF SCIENCE™

Selection of our books indexed in the Book Citation Index  
in Web of Science™ Core Collection (BKCI)

Interested in publishing with us?  
Contact [book.department@intechopen.com](mailto:book.department@intechopen.com)

Numbers displayed above are based on latest data collected.  
For more information visit [www.intechopen.com](http://www.intechopen.com)



# Role of rare-earth elements in the technology of III-V semiconductors prepared by liquid phase epitaxy

Jan Grym, Olga Procházková, Jiří Zavadil and Karel Žďánský  
*Institute of Photonics and Electronics  
Academy of Sciences CR, v.v.i.  
Czech Republic*

## 1. Introduction

First applications of rare-earth (RE) elements in semiconductor technology are rooted in radiation tolerance improvements of silicon solar cells and purification of GaP crystals. The idea was later adopted in the technology of germanium and compound semiconductors. Since the 1980's, considerable attention has been directed towards REs applications in III-V compounds both for epitaxial films and bulk crystals (Zakharenkov et al., 1997).

The uniqueness of REs arises from the fact that the lowest-energy electrons are not spatially the outermost electrons of the ion, and thus have a limited direct interaction with the ion's environment. The shielding of the 4f electrons by the outer filled shells of 5p and 5s electrons prevents the 4f electrons from directly participating in bonding (Thiel et al., 2002). The RE ions maintain much of the character exhibited by a free ion. This non-bonding property of the 4f electrons is responsible for the well-known chemical similarity of different REs. Since transitions between the electronic states of the shielded 4f electrons give rise to spectrally narrow electronic transitions, materials containing REs exhibit unique optical properties. By careful selection of the appropriate ion, intense, narrow-band emission can be gained across much of the visible region and into the near-infrared (Kenyon, 2002). Inspired by the striking results accomplished in the field of optical amplifiers and lasers based on RE-doped fibres (Simpson, 2001), substantial research activity has been recently carried out on RE-doped semiconductor materials for optoelectronics (Klik et al., 2001).

In most cases, however, achieving effective doping of III-V compounds by REs during growth from the liquid phase has proven difficult; the high chemical reactivity and the low solid solubility are the main restrictions on introducing RE atoms into the crystal lattices (Kozanecki & Groetzschel, 1990). On the other hand, the enhanced chemical affinity of REs towards most species of the shallow impurities leads to the formation of insoluble aggregates in the melt. Under suitable growth conditions, these aggregates are rejected by the growth front and are not incorporated into the grown layer: gettering of impurities takes place. Especially Si and main group-six elements acting as shallow donors in III-V semiconductors are effectively gettered due to REs high affinity towards them (Wu et al., 1992). Removal of detrimental impurities is of vital importance in applications such as PIN

photodiodes (Ho et al., 1995) or nuclear particle detector structures (Procházková et al., 2005a), where high electron and hole drift velocities are appreciated.

### 1.1 Main Objectives

Recently, we have performed a unique study of the impact of REs (Tb, Dy, Pr, Tm, Er, Gd, Nd, Lu, Ce) and their oxides ( $\text{PrO}_x$ ,  $\text{TbO}_x$ ,  $\text{Tm}_2\text{O}_3$ ,  $\text{Gd}_2\text{O}_3$ ,  $\text{Eu}_2\text{O}_3$ ) on the properties of InP layers (Procházková et al., 2002; Procházková et al., 2005a; Grym et al., 2009). This study was motivated by the lack of systematic research in the field of liquid phase epitaxy (LPE) grown III-V semiconductors from RE treated melts. REs open the door for the preparation of high purity III-V layers without extended baking of the melts or other complicated and time consuming methods. In this chapter we cover the following topics:

- Short introduction to LPE.
- Discussion of the behaviour of REs in the liquid and solid phase during LPE, their incorporation and gettering.
- Comparison of the behaviour of different RE species in the growth process of InP layers, their structural, electrical, and optical properties. InP has been chosen as a simple binary system to perform this investigation.
- Preparation of p-type InP layers, which have not been systematically investigated by other groups. Detailed description of the gettering phenomenon will be given together with the explanation of the conductivity conversion from n to p-type.
- Application of REs in the device technology: light emitting diodes (LEDs) based on InGaAsP/InP double heterostructure for near infrared spectroscopy.

## 2. Present Status

Even though numerous papers on the gettering effect of particular REs in III-V semiconductors have been published within the last three decades, no systematic study of the whole set of REs in a given III-V system has been carried out. The details of the relationship between the growth conditions, possible incorporation mechanisms, and the purifying phenomena have not been established yet.

LPE is a mature technology, which has been used in the production of III-V compound semiconductor devices for more than 40 years (Nelson, 1963); it triggered pioneering work of a vast number of semiconductor devices including LEDs, laser diodes, infrared detectors, or heterojunction bipolar transistors. LPE is capable of producing high quality layers, taking place close to thermodynamic equilibrium, with a superior luminescence efficiency and minority carrier lifetime. To emphasize several unique advantages of LPE, at least the following should be listed: (i) high growth rates; (ii) a wide range of available dopants making LPE an excellent tool for the investigation of fundamental doping studies; (iii) the low point defect densities; (iv) no toxic precursors; (v) low equipment and operating costs. Plenty of achievements ranking LPE first in the world are summarized in the review paper of Kuphal (Kuphal, 1991). However, in recent years, LPE has fallen into disfavour, especially in device applications that require large-area uniformity, extremely thin layers, abrupt composition control, and smooth interfaces. Superlattices, quantum wells, strained layers, or nonisoperiodic structures with a high lattice mismatch, all of these are grown by molecular

beam epitaxy (MBE) or metal organic vapour phase deposition (MOVPE) (Capper & Mauk, 2007). LPE has nearly disappeared from universities so that the know-how exists in the industry only and papers on LPE are scarce. Still, lots of niches in semiconductor technology remain to be served by LPE. We believe that LPE growth from RE treated melts is one of them.

LPE growth is typically carried out from supersaturated solutions composed of source materials in a graphite boat. The boat is placed in a quartz reactor tube in the atmosphere of high purity hydrogen. There are several sources of impurities that may be introduced into the grown layer (Dhar, 2005):

- Source materials and chemicals to clean them.
- Parts of the graphite boat being in contact with the growth solution.
- Contaminants deposited on the inner wall of the quartz reactor tube. These contaminants can be transported to the solution by the ambient gas during high temperature growth.
- The carrier hydrogen gas itself.
- Tools and containers for storing, handling, and cleaning the substrate and source materials.

Several procedures help to prevent these impurities to be incorporated into the layer being grown. The materials for growth are of a high purity level. At present, indium is available at 6N or even 7N purity, REs typically at 3N but recently some of their oxides up to 4N+ purity. These materials, before loading into the growth boat, are thoroughly cleaned to remove the contaminated surface. The graphite boat is made of ultra high purity graphite with low porosity. The reactor tube is made of high quality quartz and the inside wall is periodically cleaned and baked-out at high temperatures. High-purity hydrogen generator or palladium diffusion cell is used to guarantee high purity hydrogen flow. Typical LPE InP layers grown under these conditions possess electron concentrations above  $10^{17} \text{ cm}^{-3}$  at room temperature. In addition to the above self-evident precautions, there are several methods to suppress residual impurity concentrations (Rhee & Bhattacharya, 1983; Kumar et al., 1995):

- Prolonged baking of the growth solution above the growth temperature. A long bake-out under the dry hydrogen atmosphere leads to the removal of volatile impurities such as Zn, Mg, Cd, Te, and Se from the In melt by the evaporation. However, S is only partly removed due to the formation of In-S compounds and Si remains due to its low vapour pressure.
- Introduction of controlled amounts of  $\text{H}_2\text{O}$  in the growth ambient. Si is oxidized and thus prevented from being incorporated into the epitaxial layer in the electrically active form. However, this method can lead to inferior surface morphology and creation of oxygen-related traps.
- Extended prebaking of the melt can be alternatively realized in high vacuum generally leading to suppressed S concentrations.
- Other improvements including growth in  $\text{PH}_3$  atmosphere or use of dummy substrates as the source material.
- And finally, the addition of REs acting as effective gettering agents.

A brief review of REs studied in connection with III-V semiconductors prepared by LPE follows. Emphasis is put on InP and InP-based compounds. The review is sorted by individual REs. Among the REs investigated in InP, only ytterbium atoms occupy exclusively one type of the lattice site in InP. The Yb impurity in InP was proved to be incorporated as a cubic  $\text{Yb}^{3+}$  ( $4f^{13}$ ) centre on cation site (In) by Rutherford backscattering spectroscopy (Kozanecki & Groetzschel, 1990). This means that its luminescent properties are independent of the growth and doping techniques.

It is not surprising that Yb was probably the most intensively studied RE in the context of III-V compounds. In 1981, Zakharenkov reported Yb-related luminescence band in LPE grown InP (Zakharenkov et al., 1981). Further studies of RE activated luminescence in Yb and Er implanted InP, GaP, and GaAs were performed by Ennen (Ennen et al., 1983). LPE InP:Yb layers were prepared by Korber group (Korber et al., 1986). High doping levels and high growth temperatures were applied to increase Yb solubility. Employing low concentration of Yb in the melt, its gettering effect was demonstrated and high purity samples were prepared. The same group fabricated a light-emitting diode based on InP:Yb LPE layer showing intense emission at 1000 nm due to the intracentre transition of  $\text{Yb}^{3+}$  ions. (Haydl et al., 1985). Later, excitation and decay mechanisms of the  $\text{Yb}^{3+}$  in InP LPE layers were studied (Korber & Hangleiter, 1988). Nakagome confirmed incorporation of Yb in LPE InP layers by SIMS. Only a negligible portion of Yb was uniformly dispersed, most of Yb was embedded as micro-particles of Yb oxides and phosphides (Nakagome et al., 1987). He also observed deterioration of the surface morphology at higher Yb concentrations and growth temperatures. Kozanecki studied lattice location and optical activity of Yb in III-V compounds (Kozanecki & Groetzschel, 1990). He proves rather exceptional behaviour of Yb in InP consisting in relatively easy substitution of In by Yb. He states that this behaviour is related to similar ionic radii between  $\text{Yb}^{3+}$  and  $\text{In}^{3+}$  minimizing the elastic strain energy generated by the impurity, and the partially covalent Yb-P bonding. Novotný showed gettering effect of Yb in InP LPE layers (Novotný et al., 1999). The PL spectra of the studied samples were markedly narrowed and  $\text{Yb}^{3+}$  sharp intracentre transitions occurred. Different concentrations of Yb led to the preparation of both n- and p-type conductivity layers. Recently published paper (Krukovsky et al., 2004) deals with growth of GaAs prepared from Yb treated melts and demonstrates its gettering effect.

Optoelectronic materials doped with erbium atoms have received extensive attention due to their impact on optical communication systems operating at 1540 nm. Luminescent properties of erbium in III-V semiconductors were summarized in a review paper of Zavada (Zavada & Zhang, 1995). More recent review of rare-earth doped materials for optoelectronics can be found in the paper of Kenyon (Kenyon, 2002). Investigation of Er doping of InP prepared by LPE was performed by Chatterjee (Chatterjee & Haigh, 1990). Prevention of erbium oxide and hydride formation to suppress development of erbium precipitates is discussed in detail. Together with a vast number of papers on Er doped semiconductors, several papers also discuss Er gettering properties. Wu examined effect of Er admixture on structural, electrical, and optical properties of InGaAsP grown by LPE. He reports significantly diminished carrier concentrations ( $3 \times 10^{15} \text{ cm}^{-3}$ ) and a mirror-like surface morphology up to certain Er concentration limit (Wu et al., 1992). This work is further extended by PL studies of these samples (Chiu et al., 1993). Other paper of Wu reports on preparation of very high purity InP by LPE using Er gettering (Wu & Chiu, 1993). High quality of the layers is demonstrated by narrowing of the PL peaks and by the Hall

effect measurements resulting in lowered electron concentrations to  $5 \times 10^{14} \text{ cm}^{-3}$  when introducing an optimum amount of Er into the growth solution. Ho and Wu took advantage of the high purification efficiency in the fabrication of a PIN mesa photodiode, where the GaInAs absorbing layer was prepared from Er treated melts (Ho et al., 1995). In 1996, Gao gave a detailed survey on the preparation of InGaAs using Yb, Gd, and Er treated melts. Free carrier concentration reaches  $1 \times 10^{14} \text{ cm}^{-3}$ . However, this extremely low concentration is attributed to a large degree of compensation.

Further investigations were performed on Ho and Nd treated InP and GaInAsP LPE layers (Procházková et al., 1997; Procházková et al., 1999). A high donor gettering efficiency was demonstrated. Detailed studies of the gettering effect of n-type InP layers were performed by Zavadil (Zavadil et al., 1999) and Žďánský (Žďánský et al., 1999). Žďánský determined donor and acceptor concentrations from temperature variation of resistivity and Hall coefficient, and room temperature capacitance-voltage measurements. Two types of donors and an acceptor were taken into account.

Lee prepared Nd-doped AlGaAs by LPE (Lee et al., 1996) in order to apply these layers in Nd:AlGaAs lasers or LEDs with wavelength 0.91, 1.08 and 1.35  $\mu\text{m}$ . He reports mirror-like surface morphologies up to 0.4 wt% of Nd in the growth solution and uniform distribution of Nd in AlGaAs layers as well as effective gettering of residual impurities. However, higher amounts of Nd in the growth melt lead to surface roughening with many defect sites, Nd forms microparticles and segregates.

Kovalenko observed  $n \rightarrow p$  conductivity conversion at 0.1 wt% of Gd admixture on the GaAs LPE layers and a decreased electron concentration  $2 \times 10^{15} \text{ cm}^{-3}$  (Kovalenko et al., 1993). A further increase of Gd concentration above 0.1 wt% slightly increases the hole concentration. The author suggests that Gd is not incorporated into the GaAs layers. The more recent paper of Gao (Gao et al., 1999) reports the growth of very pure InAs by introducing Gd into the growth melt. Gao stresses that LPE growth occurs at thermodynamic equilibrium, and in comparison with MBE or MOVPE, the resulting crystalline perfection is superior with few defects. The electron concentration is reduced to  $6 \times 10^{15} \text{ cm}^{-3}$  when optimum Gd concentration is added to the growth melt. While the surface of conventionally grown InAs layers is mirror-like, even a small admixture of Gd ( $10^{-6} \text{ mol}\%$ ) leads to deterioration of the surface morphology. The deterioration of the surface morphology is assigned to the formation of precipitates and their nodules distributed throughout the melt. In order to suppress the number of nodules deposited in the layer, a new boat design, containing two recesses, is proposed. The supplementary recess is used for a sacrificial substrate on which nodules from the melt are deposited.

Kumar reported on the role of Dy in LPE growth of InP (Kumar & Bose, 1992). He attributes the gettering effect of donor impurities to the formation of stable silicides ( $\text{Dy}_3\text{Si}_5$  and  $\text{DySi}_2$ ), sulfides ( $\text{Dy}_2\text{S}_3$ ) and tellurides ( $\text{Dy}_2\text{Te}_3$ ), which do not dissolve in the indium melt. All layers are of n-type conductivity and the electron concentration is decreased to  $4 \times 10^{15} \text{ cm}^{-3}$ . Another paper of Misprint in ligature due to oxygen in LPE grown InGaAs with Dy admixture (Kumar et al., 1995). He further states that Dy gettering not only results in decreased carrier concentration and increased mobility but also better morphology and lower etch pit density is achieved.

Reports on the gettering properties of Pr are quite scarce. Pr was studied in GaAs, InGaAs, and InP by Jiang (Jiang, 1993). He correlates a linewidth narrowing of PL spectra with an improved crystalline quality due to Pr presence in the growth melt.

REs in the semiconductor technology have been thoroughly investigated since the last quarter of the 20<sup>th</sup> century also in Russia. Studies concerning the use of rare-earth elements in the liquid-phase epitaxy of the InP, InGaAsP, InGaAs, and GaP compounds and with the fabrication of various optoelectronic and microelectronic devices and structures based on these compounds are summarized in two review articles (Gorelenok et al., 1995; Gorelenok et al., 2003).

Reports on RE oxide admixtures in the growth technology of semiconductors are limited to praseodymium oxide (Novák et al., 1989). Gettering properties of PrO<sub>2</sub> in InGaAs grown by LPE were described by Novák (Novák et al., 1991). When PrO<sub>2</sub> is directly added to the growth melt, layers of both conductivity types are grown. While at low PrO<sub>2</sub> concentrations n-type layers are prepared, higher PrO<sub>2</sub> concentrations lead to the growth of p-type layers with hole concentrations in the range of  $2 \times 10^{15} \text{ cm}^{-3}$  to  $2 \times 10^{16} \text{ cm}^{-3}$ . Transport properties of these p-type layers were examined in detail by Kourkoutas (Kourkoutas et al., 1991). Finally, studies of incorporation of Pr into the lattice of InGaAs were performed at high PrO<sub>2</sub> concentrations in the growth melt (Novák et al., 1993). Pr is incorporated in the form of inactive complexes. These complexes can be activated by thermal annealing. The activation occurs solely in a thin layer near the surface.

### 3. Experimental

A conventional sliding boat system was available for the growth of InP and InGaAsP layers by LPE. InP epitaxial layers were prepared by the supercooling technique on (100)-oriented substrates with RE or RE oxide addition to the melt. The role of growth conditions, particularly (i) the growth temperature, (ii) the cooling rate, (iii) the growth time, and (iv) the method of the growth melt preparation were investigated together with varying RE content in the melt. The initial growth temperature was altered from 600 to 660 °C with the initial supercooling of 5 to 10 °C and the cooling rate of 0.1 to 0.7 °C/min. The growth was terminated after 15 to 30 minutes. The layer thickness varied from 4 to 15 μm. Relatively thick layers were prepared due to their intended application in radiation detectors. To suppress the great affinity of REs, especially with respect to oxygen and hydrogen, it was necessary to prevent the reactive metallic RE to come into contact with the surrounding ambient at the stage before the growth. The LPE process was realized in two cycles. In the first cycle, required amounts of In and undoped polycrystalline InP were homogenized at the temperature of 700 °C for one hour in the Pd-purified hydrogen ambient. The system was cooled, and in the second cycle, pieces of RE were mechanically embedded into the melt to form the growth solution. A polished single crystal (100)-oriented semi-insulating InP:Fe or n-type InP:Sn substrate was placed in the moving part of the boat. The substrate was covered by an InP slide to suppress its thermal decomposition. The temperature was again raised to 700 °C and held constant for one hour. The system was then cooled down to the growth temperature. Just prior to growth, the substrate was etched in situ by passing the substrate below a pure In or undersaturated In-InP melt.

The supersaturation of the solution cannot be evaluated precisely. During growth, refractory compounds of phosphorus with REs (pnictides) are formed in the liquid phase (Nakagome et al., 1987). These compounds are insoluble in indium. The effective concentration of phosphorus is diminished and so is the supersaturation (Gorelenok et al., 2003). This supplementary (negative) supersaturation may vary with RE concentration in the growth

solution. Since the growth is usually performed from only slightly supersaturated solutions, this effect must be taken into consideration, especially when growing multilayer structures in order to avoid etching of the previous layer (Astles, 1990).

Structural defects were revealed by several chemical etchants. Optical microscopy with Nomarski differential interference contrast was employed to study the surface morphology and the structural defect density. Scanning Electron Microscopy (SEM) served to trace the substrate-layer interface and the layer thickness after chemical etching. Estimates of the electrical properties on the contactless samples were gained from capacitance-voltage (C-V) measurements performed with the mercury probe at room temperature. In the probe, a smaller area circular Schottky contact with the diameter of 0.3 mm and a concentric larger area annulus Schottky contact with the outer diameter of 3 mm are formed under the pressure of 20 torr. Capacitance is monitored by a bridge with the test frequency of 1 MHz. The samples prepared on SI substrates were further characterized by the temperature dependent Hall effect measurement using a home made computer controlled apparatus with high impedance inputs and a switch box in van der Pauw configuration. The current source and current sink can be individually applied to any sample contact. The error voltages are eliminated by taking eight d.c. measurements of the Hall voltage at each temperature with two directions of the magnetic field. The set-up is equipped with a closed-cycle helium cryogenic system for the temperature range 6–320 K or with a liquid nitrogen cryostat for the temperature range 80–450 K. Photoluminescence (PL) spectra were taken at various temperatures and various levels of excitation power. The low temperature measurements were performed in order to gain information on the impurity and defect states, since the thermal energy is low enough and a variety of transitions can be resolved. The experimental set-up consists of an optical cryostat, a monochromator and a detection part. The optical cryostat is based on a closed cycle helium refrigeration system and automatic temperature controller that enables measurements in the interval of 4–300 K. Photoluminescence spectra are analyzed by 1 m focal length monochromator coupled with liquid nitrogen-cooled high purity Ge detection system and/or thermoelectrically cooled GaAs photomultiplier in the spectral range 400–1700 nm. The excitation was provided by the He-Ne and Ar ion laser. The excitation densities varied in the range of 0.1–600 mW/cm<sup>2</sup> using suitable neutral density filters.

## 4. Results and Discussion

### 4.1 Structure and Surface Morphology

Most optoelectronic devices malfunction with the presence of dislocations and other structural defects. These defects cause rapid recombination of holes with electrons without conversion of their available energy into photons; nonradiative recombination arises, uselessly heating the crystal (Queisser & Haller, 1988). The number of crystallographic defects can be decreased by the optimization of the growth technique (Procházková & Zavadil, 1999). The etch pit method is an effective way to easily measure the dislocation density (Nishikawa et al., 1989). The dependence of the InP layer surface morphology and defect density on the individual REs and their concentrations was traced.

The surface morphology of most layers grown with a small addition (several tenths of weight percent) of REs was desirably smooth and mirror-like with a minimum of surface droplets. For higher concentrations, the layers become imperfect with many defect sites on



the surface. The InP layer-substrate interface—revealed on the cleaved edge by chemical etching—was flat and free of inclusions. In general, the effect of individual REs on the surface morphology, dislocation density and interface quality was similar and only slightly varied due to different solubility of REs in the growth solution. This is in contrast with the studies of Nd and Yb addition prior to the optimisation of REs addition into the growth melt. In the case of Nd admixture, the surface morphology was very rough with isolated areas associated with the growth melt droplets even at relatively low concentrations exceeding 0.1 wt% (Procházková et al., 1999).

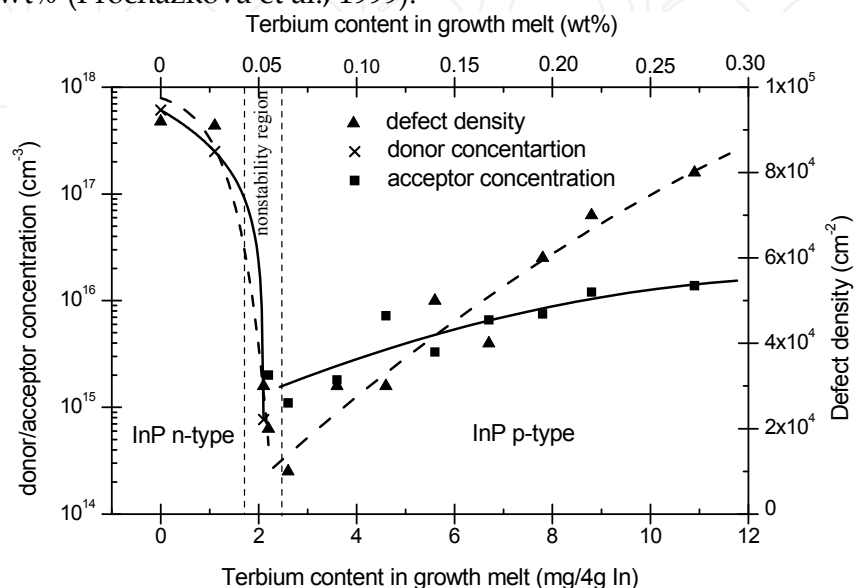


Fig. 1. Dependence of the donor/acceptor concentration of InP layer together with the density of structural defects on Tb content in the growth melt.

The layer thickness exhibited dependence not only on the temperature and the supercooling regime but also on the presence of individual REs in the melt. Again, Nd and Yb admixtures led to markedly decreased growth rates, while the other REs showed only subtle effect on the growth process. Obviously, RE oxides were employed at higher concentrations up to several weight percent—owing to their lower reactivity as compared to elemental REs—without observable deterioration of the surface morphology. The etch pit density for growth from Tb-treated melts together with impurity concentrations are depicted in Fig. 1.

#### 4.2 Electrical and Optical Properties

Firstly, REs will be divided into several groups according to their behaviour during the growth process of InP layers and their impact on electrical and optical properties of these layers. Some general observations valid for these groups of REs will be given. Thereafter, specific behaviour of particular REs will be discussed one after another.

The expected gettering effect has been observed for all REs. However, their purifying efficiency varied considerably for individual RE species. The admixture of certain REs causes not only substantial reduction of residual shallow impurities but also conversion of electrical conductivity from n to p type with one exception, that of Lu maintaining n-type conductivity even at relatively high Lu concentration reaching the solubility limit in In. Among the studied REs, only Ce was incorporated into the InP lattice.

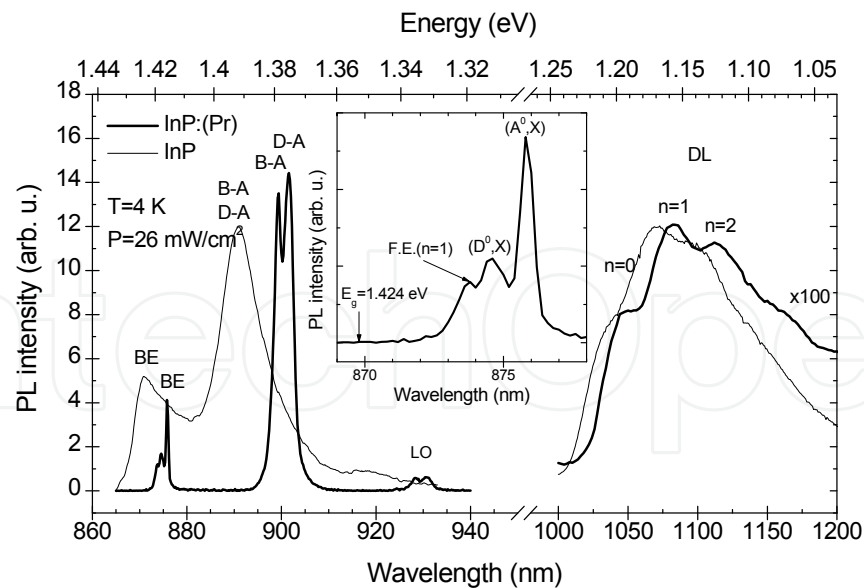


Fig. 2. Comparison of PL spectra of conventionally grown InP and p-type InP:(Pr) ( $N_A=3 \times 10^{14} \text{ cm}^{-3}$ , Pr concentration 0.3 wt%). Magnified excitonic band is shown in the inset.

A typical dependence of the shallow impurity concentration on RE content in the growth melt for Tb, Dy, Tm, Pr, and Gd (group I) is shown in Fig. 1. for the case of Tb admixture. Introduction of REs to the growth solution results in simultaneous gettering of shallow impurities. Donor impurities are preferentially gettered (Wu & Chiu, 1993). This is in accord with the well known high affinity of REs towards Si and group VI elements (Gschneidner, 1978). This preferential gettering leads to the conductivity conversion from n- to p-type. Further increase of RE addition results in moderately elevated acceptor concentrations. We claim that there are two mechanisms behind this elevation. First, new acceptor species are introduced into the growth solution with REs. The 3N purity of REs, which is currently the highest purity available on the market, is much lower than that of 6N In and InP source materials. At low concentrations of REs, the gettering effect remains virtually undisturbed. However, when RE concentration exceeds the amount necessary for the removal of all donor species, the inadvertent introduction of impurities with RE admixture to the growth solution takes place and results in elevated acceptor concentrations in the grown layers. Second, RE pnictides - particularly compounds of P and RE - are formed in the growth solution. Consequently, the stoichiometric ratio of In and P is altered at the growth interface so that the generation of P vacancies is favored (Ennen et al., 1983). The increased number of vacancies results in increased p-type activity of amphoteric impurities (Žďánský et al., 2001). Very similar behaviour could be observed for all REs oxides (group II). Clearly, for oxides, the concentration at which the conductivity conversion occurs is shifted towards higher values.

The PL spectra show fine features with narrow peaks supporting the results of C-V measurements. Typical PL spectra comparing layers grown with and without RE (Pr) admixture are shown in Fig. 2. The observed radiative transitions in studied InP samples could be grouped into three categories: band-edge (BE) transitions at about 1.418 eV (875 nm), shallow impurity related transitions at 1.38 eV (900 nm), and deep-level transitions at 1.14 eV (1090 nm) (Pearsall, 2000). There is a free space in the final line of this page.

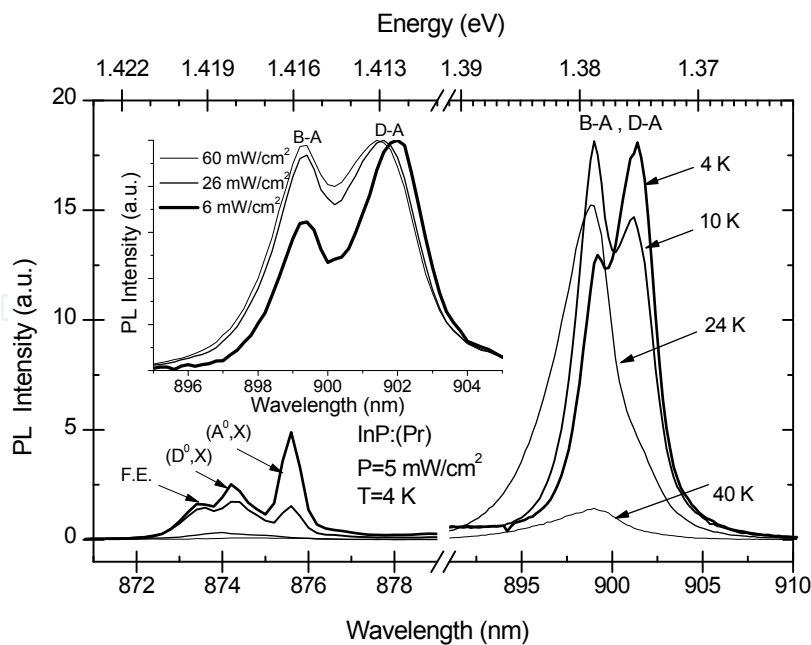


Fig. 3. Temperature dependence of NBE part of the PL spectra of p-type InP:(Pr), ( $N_A=3 \times 10^{14} \text{ cm}^{-3}$ , Pr concentration 0.3 wt%) with the inset depicting D-A peak shift with increasing excitation power.

superlinear behaviour with increasing excitation power and results from the decay of excitons. Transitions due to free exciton (FE) and excitons bound to the neutral donor ( $D^0, X$ ) or the neutral acceptor ( $A^0, X$ ) are well resolved. Transitions described as B-A and D-A are related with shallow acceptors and correspond to conduction band-acceptor and donor-acceptor pair transitions, respectively as revealed by the examination of their temperature dependence (see Fig. 3). The band of the lowest energy is rapidly quenched around 25-30 K and is thus assigned to D-A transitions. The other sub-band quenches around 70 K and is thus assigned to B-A transitions (Swaminathan et al., 1985). The peak LO is a phonon replica of the band related to shallow impurities and its position is in accordance with the known value of 43 meV for LO phonon. The peak related to shallow impurities is an unresolved convolution of (B-A) and (D-A) transitions in the case of Ce, Lu, and zero admixtures while separate peaks are well resolved at low excitation power on samples prepared with group I and group II admixtures. The D-A peak shifts with increasing excitation power (see the inset in Fig. 3) since more carriers are generated and the average distance between the donor and the acceptor undergoing the transition decreases (Hsu et al., 1994). The smaller average distance of pairs involved causes the observed blue shift of the D-A transition. The position of the D-A around 1.375 eV corresponds fairly well with the ionization energy of carbon acceptor in InP reported by Skromme (Skromme et al., 1984). Carbon probably originates from the graphite sliding boat.

The long-wavelength part of the spectra is usually dominated by Mn related band consisting of three partly resolved peaks at 1.184 eV ( $n=0$ ), 1.145 eV ( $n=1$ ), and 1.107 eV ( $n=2$ ), which are interpreted as a zero phonon line, and one, and two phonon replicas, respectively (Fig. 2). This characteristic band, observed in majority of samples, whether rare-earth treated or not, is attributed to the recombination of free or loosely bound electrons with holes bound to the Mn acceptor occupying an In site.

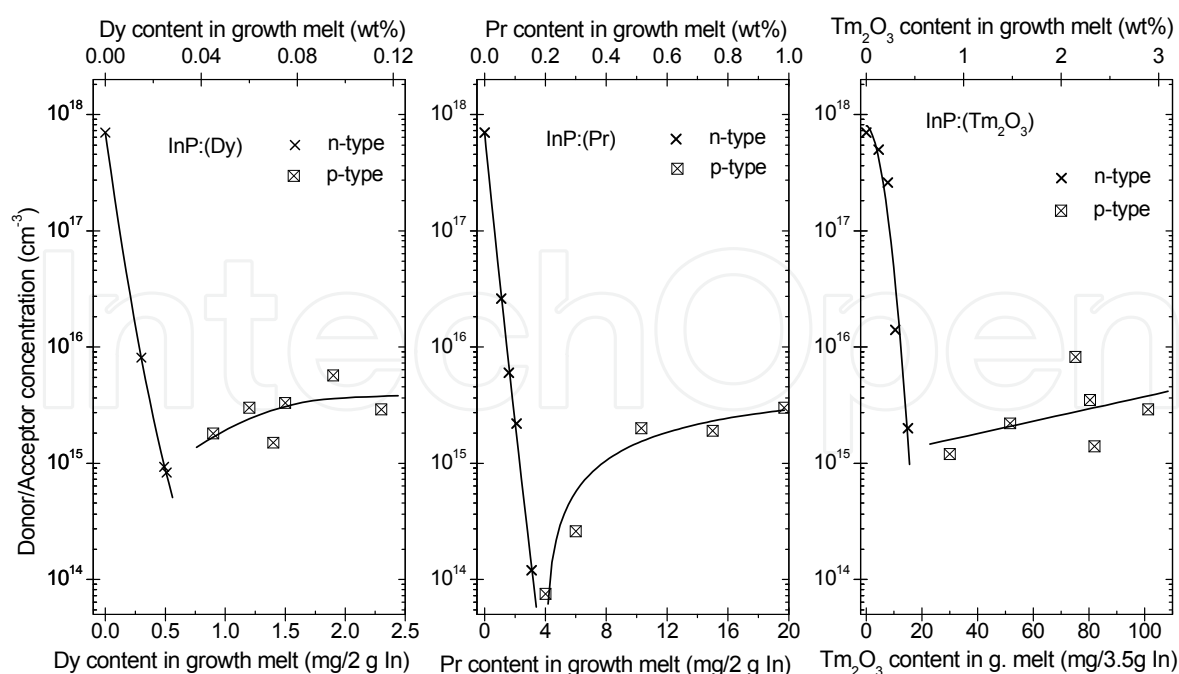


Fig. 4. Dependence of the donor/acceptor concentration of InP layer on Dy (left), Pr (middle), and Tm<sub>2</sub>O<sub>3</sub> (right) content in the growth melt.

The deep-level (DL) luminescence is strongest for conventionally grown layers (zero RE admixture). Its intensity decreases with increasing RE admixture up to some certain limit when the highest purity layers are grown and typical conductivity change occurs. Further RE increment does not have significant impact on the DL part of the spectra. These observations indicate that REs may act as scavenging agents for deep levels in addition to shallow donor gettering.

Now, specific behaviour of the individual RE elements and their oxides will be discussed.

#### 4.2.1 Terbium, Dysprosium, and Praseodymium

The shallow impurity concentration as a function of Tb concentration in the growth melt (Fig. 1) was already discussed when describing general behaviour of REs. Tb concentrations in the melt above 0.05 wt% lead to the change of the conductivity type n → p. A similar behaviour can be observed for Pr and Dy additions (Fig. 4). Only the concentration at which the conductivity change occurs is shifted towards lower (Dy) and higher (Pr) values. This is due to their different reactivity towards impurity species and their different solubility in the growth melt. Preparation of high purity p-type layers is one of the goals of our studies. From that point of view, Dy with conversion around 0.03 wt% seems to be a good candidate for the growth of p-type layers. Recall that higher concentrations of REs may deteriorate structural properties of the layers. On the other hand, Pr shows better purification efficiency, even though the n → p conversion takes place at higher RE concentration around 0.2 wt%.

The PL spectra of n and p-type InP layers prepared with the addition of Tb, Dy, and Pr were qualitatively similar in the NBE region (see Fig. 2 and Fig. 3). However, spectra are different in the spectral region above 1000 nm, where the deep level related luminescence dominates.

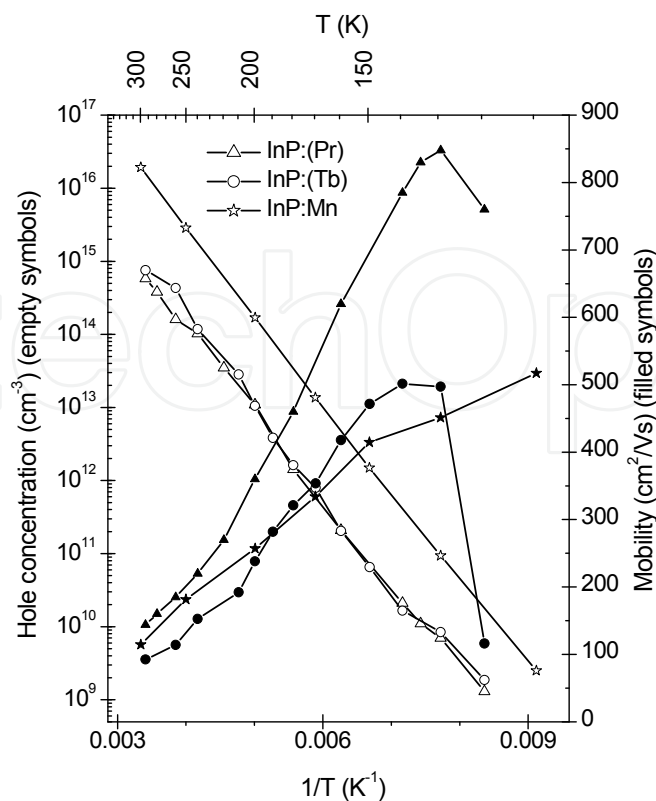


Fig. 5. Temperature dependence of the hole concentration and mobility of p-type InP:(Pr) and InP:(Tb) layers prepared on InP:Fe substrate. The curves of the same quantities of InP:Mn are shown for comparison.

To explain differences in the deep level luminescence and its origin, let us first take advantage of the Hall measurements. Fig. 5 shows curves of the hole concentration  $p$  and the hole mobility  $\mu_p$  as a function of reciprocal temperature for InP layers grown with the admixture of Pr and Tb. Data for Mn doped InP bulk crystal are also shown for comparison. The logarithmic plots of the hole concentration show straight lines in the range of several decades and are nearly identical for two different samples. Sample InP:(Tb) was prepared from the melt containing 0.07 wt% of Tb and sample InP:(Pr) with 0.25 wt% of Pr. Very similar behaviour could be observed for the layers grown with Dy. The binding energy of the dominant acceptor determined from the slope of the straight lines is equal to 0.22 eV. This value is close to the binding energy of Ge acceptor ( $210 \pm 20$  meV) and to the binding energy of Mn acceptor (230 meV) (Žďánský et al., 2002).

We already know that deep level parts of the PL spectra of the layers grown with Tb and Dy, and most of those grown with Pr admixture are dominated by the Mn band formed by the group of three peaks interpreted as a zero phonon line and its one- and two-phonon replicas (Fig. 2). Different behaviour of some of the layers grown from Pr treated melts is demonstrated in Fig. 6., where low-temperature PL spectra of Pr and Tb treated spectra are plotted for wavelength exceeding 1000 nm. The peak at 1.1952 eV is close to the estimated position of the no-phonon line (1.215 eV) of the band-Ge acceptor transitions (Žďánský et al., 2001). To sum up, the dominant acceptor responsible for  $n \rightarrow p$  conductivity conversion in InP layers grown with Tb and Dy was identified as Mn, while for some samples grown with Pr it was identified as Ge. Both Ge and Mn are residual contaminants in undoped InP and

probably become dominant electrical impurity due to the distinct preferential getting of the individual REs. Secondary ion mass spectroscopy measurements are currently under way to properly resolve this behaviour.

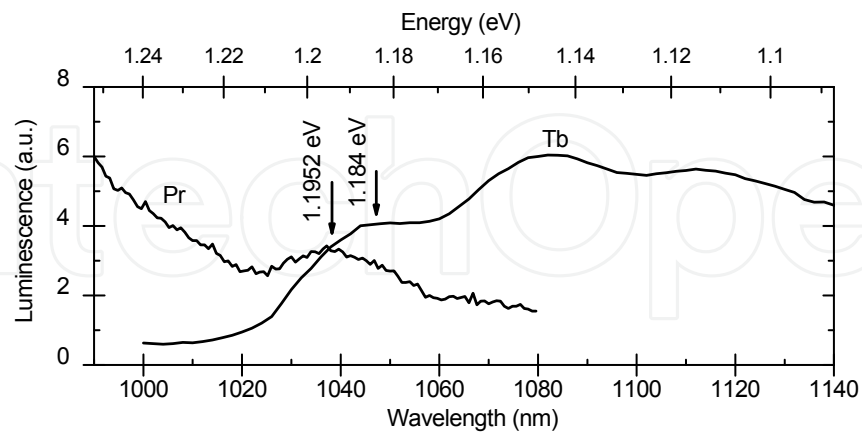


Fig. 6. InP prepared with Tb admixture showing a characteristic Mn band, and with Pr admixture with a peak at 1.1952 eV due to Ge.

Fine spectral features of the PL spectra, low donor and acceptor concentrations, and high mobilities indicate that Pr addition to the growth melts results in high purity p-type InP layers. The RT hole mobility of the InP:(Pr) sample of  $144 \text{ cm}^2/\text{Vs}$  is close to the value theoretically expected for pure p-type InP (Kranzer, 1974). Maximum mobility of  $848 \text{ cm}^2/\text{Vs}$  is reached at 130 K. This value is slightly smaller than low concentration Zn, Cd, and Mg doped p-type InP (Kuphal, 1981).

#### 4.2.2 Thulium

PL spectra of Tm treated samples show fine features in the excitonic and shallow levels related band (

Fig. 7). Measurement at low levels of excitation power enables us to distinguish three subbands within a part of the spectra associated with the shallow levels. Inspection of their temperature dependence revealed that the band of the lowest energy is rapidly quenched around 25 K and is assigned to donor-acceptor pair transitions. The other two subbands quench around 60 K and are due to conduction band-acceptor transitions. Recall similar behaviour of temperature dependence for Pr sample (Fig. 3). The two B-A subbands are tentatively assigned to Cd and Zn (Pearsall, 2000).

Sample Tm-14 (0.09 wt% of Tm) was grown on a semi-insulating (SI) InP:Fe substrate and instead of  $n \rightarrow p$  conductivity change, transition to SI state was observed. Similarly, all other samples with different Tm concentrations were converted to SI state. For that reason, electrical properties were evaluated only by using mercury probe on the samples prepared on InP:Sn substrates (Table 1). Notice that certain admixtures (around 0.08 wt%) lead to the preparation of high purity samples. The conductivity change occurs at relatively uncertain value of Tm addition. The transition to semi-insulating state related to the diffusion of Fe into adjacent InP layer is an undesirable effect. Fast out-diffusion of iron doped SI InP substrates enhanced by the presence of zinc, cadmium, and beryllium was reported and possible mechanisms of iron-acceptor exchange and acceptor interstitial leakage was

proposed (Kazmierski et al., 1992). Iron redistribution is extremely fast in adjacent p-type material, while no significant diffusion into n-type material occurs.

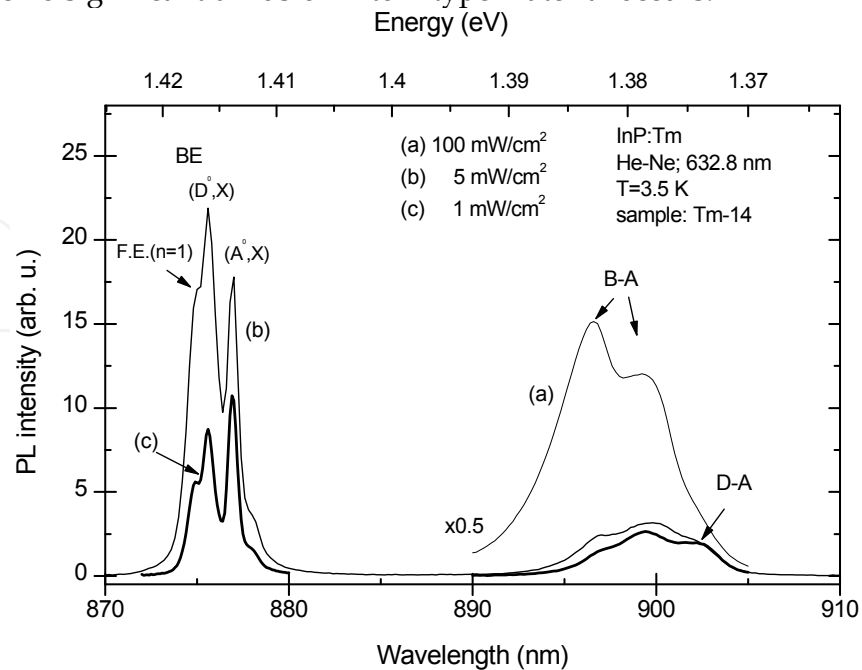


Fig. 7. NBE part of the PL spectra of p-type InP prepared with Tm admixture showing fine spectral features.

The experiments with different REs reveal the indeterminateness in the behaviour of iron in contact with p-type layers prepared from the solutions with REs admixtures. As for the layers prepared with Tb, Dy, Pr, and Ce, no iron diffusion has been observed, while samples prepared with Tm and also Gd admixtures were converted to the SI state. On the contrary, the behaviour of typical p-type dopants (Zn, Cd, Be) was universal (Kazmierski et al., 1992). This leads to the suggestion that only Tm and Gd act in the same way as a typical p-type dopant. The proposed mechanism involves an acceptor interstitial out diffusion from the p-type material into the SI substrate. The vacancy equilibrium is shifted in p-type layer leading to the excess of the phosphorus vacancy concentration, and thus, enables a higher incorporation ratio of the substitutional Fe (Procházková et al., 2005b). The iron redistribution can be well suppressed by inserting a thin buffer layer of undoped InP. The absence of significant iron diffusion through the buffer layer was validated by C-V measurements and PL spectroscopy. However, insertion of the buffer layer does not solve the problem of the Hall effect measurement requiring SI base.

#### 4.2.3 Gadolinium

Gd treated samples show extremely low concentration at which the  $n \rightarrow p$  conversion occurs (see Table 2). This observation is a proof of a high Gd reactivity (Zakharenkov et al., 1997). The PL spectra show some interesting features in the NBE part leading to the suggestion that donor impurities are gettered extremely successfully. On the other hand, high acceptor concentrations in p-type layers with relatively low admixtures are probably caused by the introduction of new impurities to the melt with Gd. However, these suggestions must be

proved by further studies. As stated above, Gd admixture leads to conversion to SI state when preparing layers on InP:Fe substrate.

sample	REC (mg)	REC (wt%)	CT	N <sub>D</sub> or N <sub>A</sub> (cm <sup>-3</sup> )	sample	REC (mg)	REC (wt%)	CT	N <sub>D</sub> or N <sub>A</sub> (cm <sup>-3</sup> )
Tm-2	1.1	0.031	n	3.0E+16	Gd-10	0.3	0.008	n	2.0E+15
Tm-15	2.7	0.077	n	1.0E+15	Gd-16	0.4	0.011	p	3.5E+15
Tm-7	2.8	0.080	n	7.4E+14	Gd-12	0.5	0.014	p	7.7E+15
Tm-9	2.8	0.080	p	8.9E+14	Gd-11	1.0	0.028	p	6.3E+15
Tm-36	2.9	0.083	p	4.2E+15	Gd-14	2.1	0.059	p	1.2E+16
Tm-6	3.2	0.091	p	1.0E+15	Gd-15	5.0	0.141	p	2.2E+16

Table 1. Donor (acceptor) concentrations of the samples prepared with Tm and Gd admixture. REC stands for RE concentration, CT for conductivity type.

#### 4.2.4 Cerium

As stated in the introductory part of this section, Ce is the only element among the studied ones, which was incorporated into the InP lattice. In our earlier studies of Yb admixture (not included in this review) it was shown that Yb was incorporated into the InP lattice, layers exhibit n→p conductivity conversion and Yb itself was identified as the dominant acceptor responsible for the conductivity crossover (Žďánský et al., 2002). To give evidence of this statement, let us first look at the left panel of Fig. 8 showing the acceptor concentration as a function of Ce content in the melt. All layers, even those prepared at very low Ce concentration, are of p-type conductivity. When increasing the Ce concentration, the acceptor concentration in the layers is also increased. This may imply that Ce behaves as an acceptor itself. It was recently shown that dominant acceptors responsible for the n→p conductivity conversion of the LPE InP:Yb layers are Yb<sup>3+</sup> ions incorporated into the InP lattice as a cubic Yb<sup>3+</sup> center on the cation site (In) (Žďánský et al., 2002). Typical temperature dependence of the hole concentration and mobility derived from the Hall measurements for p-type InP layers doped with Ce is shown in the right panel of Fig. 8. The data for Yb doped LPE layers and Zn doped bulk crystals are given for comparison. Similar behaviour of the layers doped with Yb and Ce can be clearly seen. Hall measurements presented in Fig. 8 have been performed in the range from room temperature to about 35 K. Below this threshold temperature, the conductivity of Ce and Yb doped samples changes very slowly so that the temperature equilibrium cannot be reached within hours. A slow decay of conductivity is initiated at about 60 K. The samples doped with Yb and Ce reach a metastable state and results of Hall measurements are not reliable any more. Introducing Ce and Yb into the InP lattice, their atoms are exposed to a strong electron-lattice interaction due to their large atomic radii and due to a large difference between electronegativities of Yb, Ce, and In (Zavadil et al., 2007). A potential barrier raised by this interaction is supposed to be responsible for the observed metastability of electrical conductivity (Procházková et al., 2005c). The curves of the hole concentration reveal straight lines at low temperatures giving the binding energy of Ce equal to 31 meV.



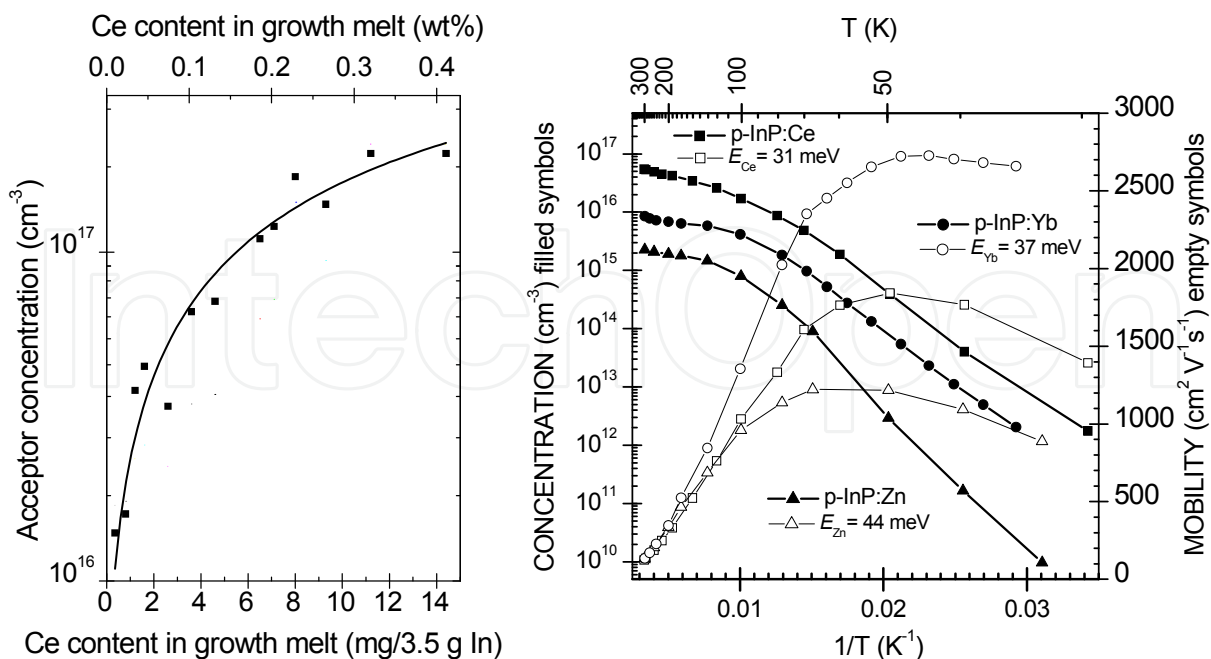


Fig. 8. Dependence of the acceptor concentration on Ce content in the growth melt (left panel) and temperature dependence of the hole concentration and mobility of p-type InP layers doped with Ce, Yb, and Zn (right panel).

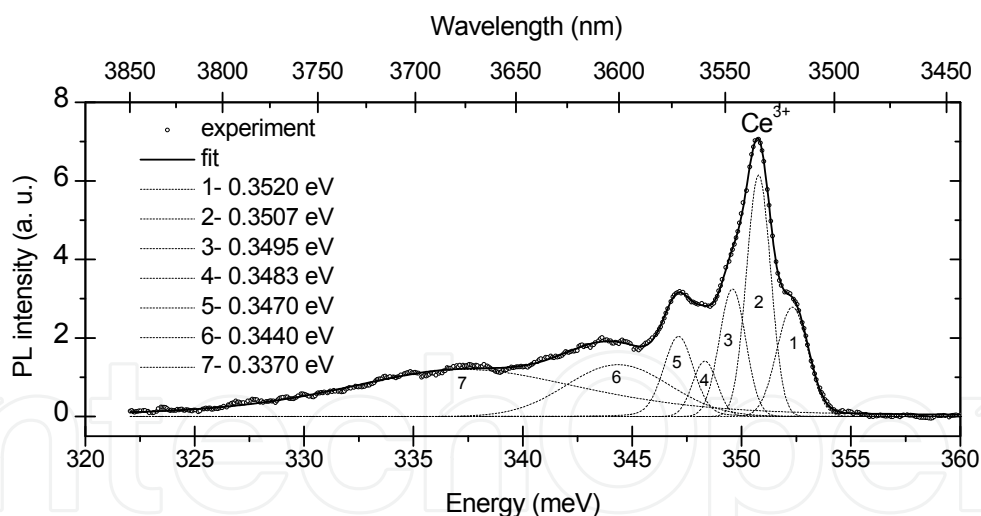


Fig. 9. PL spectrum of the InP layer prepared with Ce admixture.

Among the other REs, Ce and Yb have relatively simple energy level scheme of 4f shell with only one excited state. Their position within the lanthanide series can be viewed as complementary; Ce<sup>3+</sup> possesses one 4f electron, while Yb<sup>3+</sup> possesses thirteen 4f electrons. The PL spectrum of InP:Ce (0.2 wt%) layer measured in the mid-infra-red range is shown in Fig. 9. The sharp inner shell 2F<sup>7/2</sup> → 2F<sup>5/2</sup> transition of Ce<sup>3+</sup> ion at 3534 nm (0.3507 eV) together with a fine structure caused by crystal field splitting is clearly seen. This is a direct proof of Ce<sup>3+</sup> ions being incorporated into the InP lattice.

#### 4.2.5 Lutetium

Samples prepared with with the admixture of Lu were of n-type conductivity at any Lu concentration. A list of results of C-V measurements for selected samples follows: sample LuI-1 (0.014 wt%) with  $N_D=3.5 \times 10^{17} \text{ cm}^{-3}$ ; sample LuI-2 (0.049 wt%) with  $N_D=1.7 \times 10^{17} \text{ cm}^{-3}$ ; sample LuI-4 (0.108 wt%) with  $N_D=3.4 \times 10^{16} \text{ cm}^{-3}$ ; and sample LuI-6 (0.173 wt%) with  $N_D=8.8 \times 10^{15} \text{ cm}^{-3}$ . Higher Lu concentration could not be applied due to the deterioration of the surface morphology.

Let us briefly sum up the effect of the studied REs on electrical and optical properties of the InP layers. Dy produced the conductivity conversion from n→p at the lowest concentration. Pr and Tm addition resulted in high purity samples. Typical Pr treated samples exhibited high mobilities. The fine spectral features in the NBE part of the spectra were described on Pr and Tm treated samples. The dominant impurity in the case of p-type layers were determined as Ge or Mn for Pr treated samples, Mn for Tb and Dy samples, and Ce itself for Ce samples. The temperature dependent Hall effect measurement could not be performed on the samples with Tm and Gd admixture due to their conversion to SI state caused by Fe out-diffusion from the InP:Fe substrate. Finally, Lu did not exhibit as large an impact as the other elements and its addition always resulted in the growth of n-type layers.

REs show high oxidation potential and therefore must be handled carefully in the atmosphere with an oxygen content (Korber et al., 1986). The insertion of partially oxidized REs into the growth solution may cause difficulties. REs are inert towards hydrogen atmosphere. However, this holds only for room temperature. At the temperature above 300 °C, the pure REs absorb hydrogen instantly and create very stable hydrides. The extent of the hydride formation is practically limited by the previous oxidation of the pure RE metal (Novák et al., 1991). It follows that the gettering effect is extremely sensitive to the RE oxide and hydride formation. The alteration of this ratio from run to run causes the deterioration of the reproducibility of the epitaxial growth process. Taking into account certain level of uncertainty in the behavior of the elemental REs, from now on, the role of RE oxides will be discussed.

#### 4.2.6 Thulium oxide

The standard two-period cycle for the sample preparation did not lead to a substantial improvement of the layer quality. Namely, its background concentrations were not decreased significantly. Thus, a four-period cycle of the sample preparation was proposed. During the first two periods, solution of In and  $\text{Tm}_2\text{O}_3$  was prepared and homogenized at the temperature of 730 °C. In the third period, InP was added and shortly homogenized again. The last period was a standard growth period as described in section describing experimental procedures. Very similar impact of  $\text{Tm}_2\text{O}_3$  in comparison with elemental thulium was observed. The expected lower reactivity of the oxide results in much larger value of concentration (around 0.5 wt%) at which the conductivity crossover is observed (Fig. 4). PL spectra allowed to distinguish the B-A transitions from D-A pair ones, and enabled identification of exciton related transitions. Similarly to Tm treated samples, threesubbands are typically resolved in the shallow levels related part of the spectra (left panel of Fig. 10).

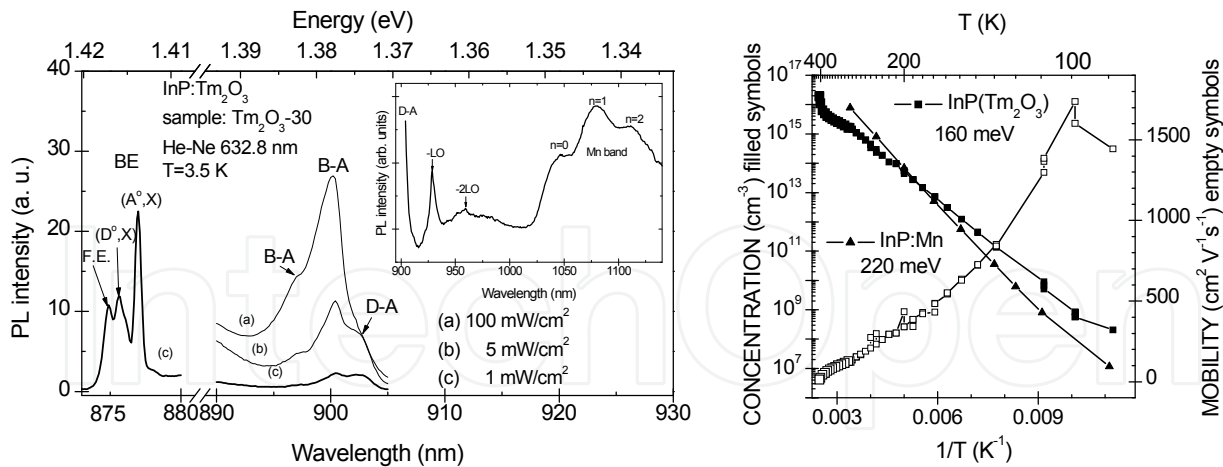


Fig. 10. NBE part of the PL spectra of p-type InP prepared with  $\text{Tm}_2\text{O}_3$  admixture showing fine spectral features with the inset depicting its long wavelength part (left panel) and Hole concentration and mobility of p-type InP layers grown with  $\text{Tm}_2\text{O}_3$  admixture (right panel).

Hole concentration and mobility of the layers are given in the right panel of Fig. 10 together with corresponding data measured on InP:Mn sample for comparison. The binding energy of the dominant acceptor responsible for  $n \rightarrow p$  conductivity conversion was determined as 160 meV. Low temperature PL spectra (see the inset in the left panel of Fig. 10) exhibit a broad band at 960 nm (1.29 eV) that fairly well corresponds with the above mentioned energy. The origin of this impurity is not clear. The sample with  $\text{Tm}_2\text{O}_3$  ( $\text{Tm}_2\text{O}_3$ -30, 2.3 wt%) is characterized by the following values of free carrier concentration and mobility:  $p(300) = 1.7 \times 10^{15} \text{ cm}^{-3}$ ,  $\mu(300) = 127 \text{ cm}^2 \text{ V}^{-1} \text{ s}^{-1}$ . Maximum mobility  $\mu(100) = 1764 \text{ cm}^2 \text{ V}^{-1} \text{ s}^{-1}$  is reached at the temperature of 100 K.

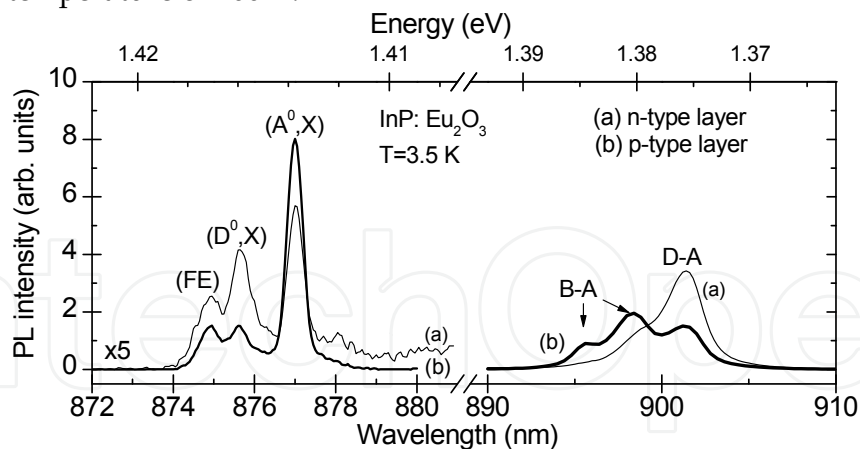


Fig. 11. NBE part of the PL spectra of both n-type and p-type InP prepared with  $\text{Eu}_2\text{O}_3$  admixture

#### 4.2.7 Europium oxide

Europium oxide appears to have a very high purification effect. Unfortunately there is no strict level of  $\text{Eu}_2\text{O}_3$  at which the conductivity change takes place. The choice of substrate seems to play an important role. Two n-type layers of very low donor concentration were grown on InP:Fe substrate:

sample EuO-6 (0.39 wt%) with  $N_D=2.5 \times 10^{14} \text{ cm}^{-3}$

sample EuO-15 (1.13 wt%) with  $N_D=1.2 \times 10^{14} \text{ cm}^{-3}$

The corresponding layers prepared on InP:Sn substrate are of both n-and p-type:

sample EuO-7 (0.49 wt%, n-type) with  $N_D = 1.1 \times 10^{15} \text{ cm}^{-3}$

sample EuO-19 (1.49 wt%, p-type) with  $N_A = 2.6 \times 10^{15} \text{ cm}^{-3}$

A further series of experiments has to be performed to clarify the behaviour of  $\text{Eu}_2\text{O}_3$  and its relation to the substrate properties. The PL spectra show fine features with narrow peaks supporting the results of C-V measurements. The NBE part of the spectra clearly demonstrates differences between n-type and p-type layers.

#### 4.2.8 Other oxides

To round off the enumeration of RE oxides,  $\text{PrO}_x$ ,  $\text{Gd}_2\text{O}_3$ , and  $\text{TbO}_x$  admixtures have to be mentioned. These samples were characterized by the C-V measurements. The data are summarized in Table 2 (asterisk means different conditions of the sample preparation).  $\text{PrO}_x$  samples were further characterized by PL measurements. The behavior of  $\text{PrO}_x$  did not markedly differ from the behavior of elemental Pr. Evidently, the conductivity conversion arose at higher concentration around 1 wt%. Admixture of  $\text{Gd}_2\text{O}_3$  and  $\text{TbO}_x$  always resulted in preparation of n-type layers. This was probably caused by their low solubility in the In-based melt. The last sample  $\text{TbOI-6}^*$  was prepared by a four-period cycle similar to the earlier mentioned  $\text{Tm}_2\text{O}_3$  layers. Moreover, the temperature of homogenization was increased to 800 °C. To briefly sum up RE oxides show some promising advantages over the elemental REs. However, the process of their introduction into the melt and its subsequent homogenization must be solved in order to result in repetitive preparation of high quality layers.

sample	REC (mg)	REC (wt%)	CT	$N_D$ or $N_A$ ( $\text{cm}^{-3}$ )	sample	REC (mg)	REC (wt%)	CT	$N_D$ or $N_A$ ( $\text{cm}^{-3}$ )
$\text{Gd}_2\text{O}_3$ -1	1.9	0.09	n	$2.6\text{E}+17$	$\text{Nd}_2\text{O}_3$ -0	0.0	0.00	n	$2.8\text{E}+17$
$\text{Gd}_2\text{O}_3$ -2	3.1	0.15	n	$1.7\text{E}+17$	$\text{Nd}_2\text{O}_3$ -4	2.5	0.12	n	$7.1\text{E}+14$
$\text{Gd}_2\text{O}_3$ -3	15.1	0.74	n	$8.0\text{E}+16$	$\text{Nd}_2\text{O}_3$ -3	5.0	0.24	p	$3.4\text{E}+15$
$\text{Gd}_2\text{O}_3$ -4	30.0	1.46	n	$9.3\text{E}+16$	$\text{Nd}_2\text{O}_3$ -5	7.0	0.34	p	$3.0\text{E}+15$
$\text{Gd}_2\text{O}_3$ -5	60.0	2.88	n	$1.4\text{E}+16$	$\text{Nd}_2\text{O}_3$ -2	10.0	0.49	p	$3.2\text{E}+15$
$\text{Gd}_2\text{O}_3$ -8*	30.2	0.85	n	$6.8\text{E}+15$	$\text{Nd}_2\text{O}_3$ -6	15.0	0.73	p	$3.0\text{E}+15$
$\text{PrO}_x$ -8	5.0	0.25	n	$5.7\text{E}+15$	$\text{Nd}_2\text{O}_3$ -7	45.0	2.17	p	$3.9\text{E}+15$
$\text{PrO}_x$ -2	15.8	0.79	n	$2.2\text{E}+15$	$\text{TbO}_x$ -1	25.0	1.25	n	$6.6\text{E}+17$
$\text{PrO}_x$ -1	24.5	1.23	p	$2.8\text{E}+15$	$\text{TbO}_x$ -2	50.8	2.54	n	$2.3\text{E}+17$
$\text{PrO}_x$ -6	30.0	1.50	p	$2.0\text{E}+15$	$\text{TbO}_x$ -3	97.6	4.88	n	$1.3\text{E}+16$
$\text{PrO}_x$ -5	59.5	2.98	p	$3.8\text{E}+15$	$\text{TbO}_x$ -6*	49.3	2.46	n	$7.8\text{E}+15$

Table 2. Donor (acceptor) concentrations of the samples prepared with different RE oxide admixtures. REC stands for RE concentration, CT for conductivity type.

### 4.3 Towards the Application

In this section we try to demonstrate the application of the gettering phenomena in device concepts. InP-based radiation detectors and double heterostructure LEDs in the near infrared region were selected as examples.

#### 4.3.1 Radiation Detectors

While the mainstream of research effort in the area of semiconductor technology is nowadays aimed at producing nanometer-thin structures, there remain niches, such as fabrication of radiation detector structures, where relatively thick layers are valued and required.

InP-based materials have various advantages, such as bandgap energy suitable for light emitters in the long-wavelength region, an extremely high saturation velocity of electrons suitable for the active channel in high-power and high-speed electronic devices, as well as high thermal conductivity and high threshold of optical catastrophic degradation (Wada & Hasegawa, 1999). On the other hand, InP-based materials are less mature in wafer- and device-processing technologies such as surface passivation, metal-semiconductor gate technology or ohmic contact preparation. New studies and developments are required in various fields of technology to fully exploit the intrinsic advantages of InP.

InP single crystals are promising materials for the preparation of radiation detectors operating at room temperature. The room temperature operation is possible due to sufficiently wide bandgap energy  $E_g=1.35$  eV at room temperature and high mass density  $\rho=4.8$  g/cm<sup>3</sup>. The high value of atomic number of In ( $Z_{In}=49$ ) predicates high stopping power, which is proportional to  $Z^n$  ( $n\approx 4-5$ ) for a high energy photon (Pelfer, 2001). Preparation of thick high-purity InP layers would be appreciated to exploit the above mentioned potential in radiation detectors. High purity and homogeneity of the layers is essential to attain large charge collection efficiency. Conventionally prepared bulk and epitaxial InP crystals are of n-type conductivity due to intrinsic donor impurities. Intentional doping with shallow acceptors is generally the way to prepare p-type material. In this chapter, we have demonstrated that the application of certain concentration of appropriate RE leads to the preparation of high purity InP of both conductivity types without intentional doping.

High purity InP layers of both n- and p- type conductivity with carrier concentration diminished to  $10^{14}$  cm<sup>-3</sup> thanks to Pr additions to the growth melts were used to fabricate detector structures with p-n junction. High purity n-type and the p-type layers were subsequently grown on Sn doped n-type substrate. Each of the layers was 10  $\mu$ m thick. Metal contacts were deposited by vacuum evaporation: Au-Be/Cr/Au contacts on p-type InP and AuGeNi contacts on n-type InP. The structures were diced into chips of 500x500  $\mu$ m. Spectra of  $\alpha$ -particles from the <sup>241</sup>Am source of 5.48 MeV were measured at room temperature in vacuum with negative voltage on the irradiated (p-type InP) side. The highest achieved CCE was 40 % with FWHM energy resolution of 8 % (Procházková et al., 2009).

#### 4.3.2 Double Heterostructure LEDs

InP itself had not received much interest until it was used as a substrate for InGaAsP-based LEDs and lasers (Hsieh et al., 1976) and InGaAs transport devices (Takeda et al., 1976).

Lattice matched InGaAsP to InP substrate can cover the energy range from 0.75 eV to 1.35 eV at RT. This energy range is important in silica-fibre-based optical communications and infrared spectroscopy (Rakovics et al., 2002). We demonstrate the purifying effect of Pr on the preparation of InGaAsP layers and InGaAsP/InP double heterostructure LEDs by liquid phase epitaxy. Background impurities in the active region, especially at high concentrations, introduce defects that act as recombination centres. High background concentration may also lead to carrier spill-over into one of the confinement regions and decrease the radiative efficiency.

Four-layer structures were grown consisting of an n-type buffer layer (7  $\mu\text{m}$ ), Pr-treated InGaAsP active layer (400 nm), p-type InP:Zn confinement layer (2  $\mu\text{m}$ ), and p-type InGaAsP:Zn contact layer. Ohmic contacts were deposited by vacuum evaporation: Au-Be/Cr/Au contacts on p-type InGaAsP and AuGeNi contacts on n-type InP. Electrical and optical properties were evaluated on the chips with the size of 500 $\times$ 500  $\mu\text{m}$ , PL spectra were measured on the samples without p-type confinement and contact layer.

Narrowing of the PL peak at RT was observed already when 0.1 wt% Pr admixture was applied. The FWHM dropped from 48 meV for a conventionally grown layer to 42 meV for the layer grown with 0.1 wt% of Pr. Narrowing of the peak is caused by the elimination of a donor band, which - in the case of heavily doped material - extends into the conduction band and gives rise to the peak broadening and shifting towards lower energy (Kasap, 2001). The RT electroluminescence spectral bandwidth measured at 10 mA was 57 meV. Typical external quantum yield of the fabricated LEDs was 1.7 % and integrated optical power was 1.8 mW, both measured at RT and electrical current of 100 mA.

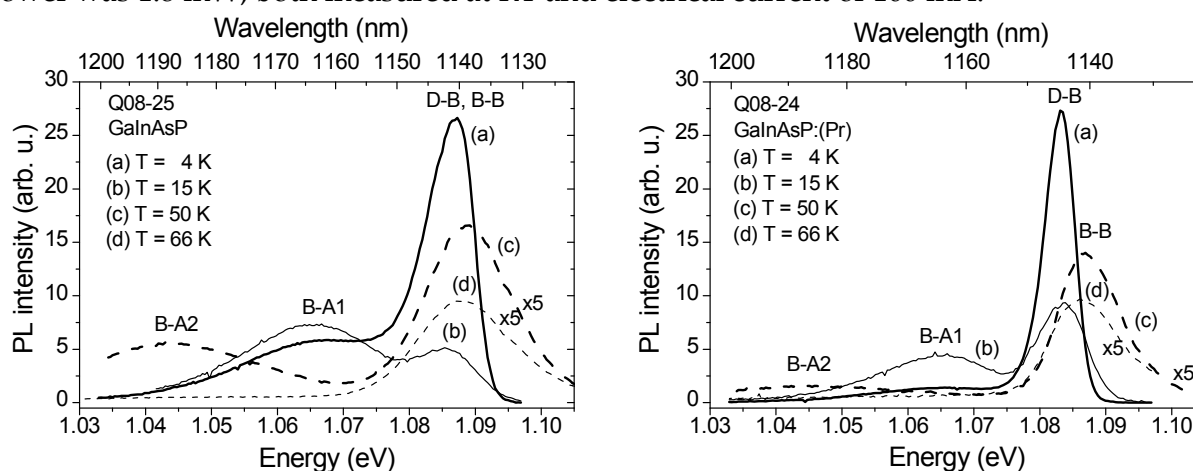


Fig. 12. Low temperature PL spectra of InGaAsP (left panel) and InGaAsP:(Pr) (right panel) are shown for temperatures 4, 15, 50 and 66 K by curves (a), (b), (c) and (d), respectively.

InGaAsP layers with different amounts of Pr admixture, corresponding to impurity concentrations of  $1.6 \times 10^{17} \text{ cm}^{-3}$  (0 wt% of Pr),  $1.2 \times 10^{17} \text{ cm}^{-3}$  (0.15 wt% of Pr),  $9.2 \times 10^{16} \text{ cm}^{-3}$  (0.2 wt% of Pr), and  $5.4 \times 10^{15} \text{ cm}^{-3}$  (0.5 wt% of Pr), were further investigated by low temperature PL spectroscopy. PL spectra of conventionally grown InGaAsP layer (i.e. without Pr addition) measured at four temperatures are shown in the left panel of Fig. 12. Temperature dependence of PL spectra was investigated in the temperature range 4–70 K in order to deduce contributions from various radiative transitions. The dominant band (D-B, B-B) at the lowest temperature of 4 K is at 1.084 eV with the halfwidth of 10 meV. The

contributions from free or bound excitons, band to band (B-B) and shallow donor to valence band (D-B) transitions are not resolved. With increasing temperature, in the range 4–70 K, the band is broadened and slightly shifted but individual contributions are still not resolved. Transitions due to shallow acceptors with binding energies (23 meV and 45 meV) could also be seen for temperatures below 70 K. When the temperature is increased above 70 K, only the broad band due to band to band transition is seen and is gradually shifted to lower energy with increasing temperature. This band is centred at 1.03 eV (1200 nm) at 280 K, and has the halfwidth of 42 meV.

All samples prepared with Pr admixture exhibit a distinct narrowing of PL spectra and D-B transition could be resolved from B-B transitions in the temperature range 4–15 K. In view of the fact that the donor binding energy  $E_D \sim 4.5$  eV is very small, the donor related band is resolved only for temperatures below 20 K in samples purified by Pr addition. Typical low temperature PL spectra of InGaAsP:(Pr) samples are shown in the right panel of Fig. 12. At the lowest temperature, the spectrum is dominated by the narrow band (D-B) with the halfwidth of 5 meV, which is due to donor to valence band transitions. When the temperature is increased above 15 K, but not exceeding 70 K, the band is shifted by about 5 meV to higher energy (B-B) and is dominated by band to band transitions.

By the inspection of Fig. 12 we can see that considerable suppression of acceptor related radiative transitions takes place in Pr treated samples. This suggests effective gettering of acceptor impurities.

## 5. Conclusions

High purity InP layers were prepared by liquid phase epitaxy. Their growth was performed from the melts containing, besides essential components, also REs (Tb, Dy, Pr, Tm, Gd, Lu, Ce) and some of their oxides ( $\text{PrO}_x$ ,  $\text{Tm}_2\text{O}_3$ ,  $\text{Gd}_2\text{O}_3$ ,  $\text{Eu}_2\text{O}_3$ , and  $\text{TbO}_x$ ). The content of individual RE species was systematically altered to investigate their impact on physical properties of the grown layers.

The expected gettering effect was observed for all REs. However, their purifying efficiency varied considerably for individual RE species. Introducing REs to the growth solution, simultaneous gettering of shallow impurities takes place. InP layers with shallow impurity concentration decreased by up to four orders of magnitude were grown. Donor impurities are preferentially gettering due to the high affinity of REs towards Si and group VI elements. The preferential gettering leads to conductivity conversion from n- to p-type when increasing RE concentration in the growth melt. Very similar behaviour could be observed for RE oxides. Due to their lower reactivity, the concentration at which the conductivity conversion occurred, was shifted towards higher values. In the case of Lu,  $\text{Gd}_2\text{O}_3$ , and  $\text{TbO}_x$  addition, all layers maintained n-type conductivity even at relatively high concentrations reaching its solubility limit in the growth melt. Among the studied REs, only Ce was conclusively incorporated into the InP lattice.

To emphasize the finest results, the addition of 0.2 wt% of Pr led to the following values of the hole concentration and mobility at room temperature:  $p(300) = 8 \times 10^{13} \text{ cm}^{-3}$  and  $\mu(300) = 144 \text{ cm}^2 \text{ V}^{-1} \text{ s}^{-1}$ . The samples showing low concentrations of residual impurities were characterized by PL spectroscopy. The observed significant narrowing of PL curves and the corresponding appearance of fine spectral features are typical characteristics of pure materials, low in defects.

With the help of temperature dependent Hall measurements and PL spectroscopy, the nature of the dominant acceptor in p-type InP was recognized. The dominant acceptor in InP layers grown with Tb, Dy, and Pr was identified as Mn. In some samples grown with Pr, Ge was a dominant acceptor. Samples prepared on InP:Fe substrates with Tm and Gd admixtures were converted to semi-insulating state. This conversion is attributed to the out-diffusion of iron from the InP:Fe substrate.

The surface morphology of the layers grown with a small addition of RE (several tenths of weight percent for elemental REs and several percent for their oxides) was desirably smooth and mirror-like with a minimum of surface droplets. Optimized admixtures of REs resulted in lowered dislocation densities.

Preliminary studies of the application of the unique properties of REs were performed. Pr has been chosen for these investigations since its admixtures (i) provoke conductivity conversion at relatively low concentrations in the melt, (ii) do not influence the growth rate, and (iii) under appropriate growth conditions lead to lowered dislocation densities and good surface morphology (Grym et al., 2009). Applications in semiconductor radiation detectors and double heterostructure LEDs were demonstrated.

*This work was supported by the projects #102/08/P617 and #102/09/1037 of the Czech Science Foundation. The authors thank M. Hamplová, Z. Podvalová, J. Zelinka, and V. Malina for technical assistance, P. Gladkov for the PL measurements of Ce doped samples, and R. Yatskiv for the measurements of the detection performance of the structures with p-n junction.*

## 6. References

- Astles, M.G. (1990). Liquid-Phase Epitaxial Growth of III-V Compound Semiconductor Materials and their Device Applications, IOP Publishing Ltd
- Capper, P. & Mauk, M., Eds. (2007). Liquid Phase Epitaxy of Electronic, Optical and Optoelectronic Materials, John Wiley & Sons, ISBN: 978-0-470-85290-3
- Chatterjee, A.K. & Haigh, J. (1990). Investigation of erbium doping of InP and (Ga,In)(As,P) layers grown by LPE, Journal of Crystal Growth, Vol. 106, pp. 537-542
- Chiu, C.M.; Wu, M.C. & Chang, C.C. (1993). Photoluminescence of undoped and Er-doped InGaAsP layers grown by liquid phase epitaxy, Solid State Electronics, Vol. 36, pp. 1101-1106
- Dhar, S. (2005). Growth of high purity semiconductor epitaxial layers by liquid phase epitaxy and their characterization, Bulletin of Materials Science, Vol. 28, pp. 349-353
- Ennen, H., et al. (1983). Rare earth activated luminescence in InP, GaP and GaAs, Journal of Crystal Growth, Vol. 64, pp. 165-168
- Gao, H.; Krier, A. & Sherstnev, V. (1999). High quality InAs grown by liquid phase epitaxy using gadolinium gettering, Semiconductor Science and Technology, Vol. 14, pp. 441-445
- Gorelenok, A.; Kamanin, A. & Shmidt, N. (1995). Rare-earth elements in the technology of InP, InGaAsP and devices based on these semiconductor compounds, Microelectronics Journal, Vol. 26, No. 7, pp. 705-723
- Gorelenok, A.; Kamanin, A. & Shmidt, N. (2003). Rare-earth elements in the technology of III-V compounds and devices based on these compounds, Semiconductors, Vol. 37, No. 8, pp. 894-914



- Grym, J., et al. (2009). LPE growth of InP layers from rare-earth treated melts for radiation detector structures, *Materials Science and Engineering: B*, pp. In Press, Corrected Proof, doi:10.1016/j.mseb.2009.03.004
- Gschneidner, K.A., Ed. (1978). *Handbook on the Physics and Chemistry of Rare-earth*, North-Holland Publishing Company, ISBN: 978-0-444-82178-2
- Haydl, W.H., et al. (1985). Ytterbium-doped InP light-emitting diode at 1000 nm, *Applied Physics Letters*, Vol. 46, pp. 870-872
- Ho, W.J.; Wu, M.C. & Tu, Y.K. (1995). High responsivity GaInAs PIN photodiode by using Erbium gettering, *IEEE Transactions on Electron Devices*, Vol. 42, pp. 639-644
- Hsieh, J.J.; Rossi, J.A. & Donnelly, J.P. (1976). Room-temperature cw operation of GaInAsP/InP double-heterostructure diode lasers emitting at 1.1  $\mu\text{m}$ , *Applied Physics Letters*, Vol. 28, No. 12, pp. 709-711
- Hsu, J.K., et al. (1994). Photoluminescence studies of interstitial Zn in InP due to rapid thermal annealing, *Journal of Vacuum Science & Technology B: Microelectronics and Nanometer Structures*, Vol. 12, No. 3, pp. 1416-1418
- Jiang, G.C. (1993). Gettering properties of praseodymium in GaAs, InGaAs and InP grown by liquid phase epitaxy, *Crystal Research and Technology*, Vol. 31, pp. 365-371
- Kasap, S.O. (2001). *Optoelectronics and Photonics: Principles and Practices*, Prentice Hall ISBN: 0201610876
- Kazmierski, C.; Robein, D. & Gao, Y. (1992). Universal iron behavior in Zn-, Cd- and Be-doped InP, *Journal of Crystal Growth*, Vol. 116, pp. 75-80
- Kenyon, A.J. (2002). Recent developments in rare-earth doped materials for optoelectronics, *Progress in Quantum Electronics*, Vol. 26, pp. 225-284
- Klik, M., et al. (2001). Optically induced Auger recombination of Yb<sup>3+</sup> in p-type InP, *Physica B*, Vol. 308-310, pp. 884-887
- Korber, W., et al. (1986). Rare earth ions in LPE III-V semiconductors, *Journal of Crystal Growth*, Vol. 79, pp. 741-744
- Korber, W. & Hangleiter, A. (1988). Excitation and decay mechanisms of the intra-4f luminescence of Yb<sup>3+</sup> in epitaxial InP:Yb layers, *Applied Physics Letters*, Vol. 52, pp. 114-116
- Kourkoutas, C.D., et al. (1991). Transport properties of praseodymium doped p-type InGaAs layers, *Solid State Communications*, Vol. 78, pp. 543-546
- Kovalenko, V.; Krasnov, V. & Malyshev, V. (1993). Gettering of donor impurities by Gd in GaAs, *Semiconductor Science and Technology*, Vol. 8, pp. 1755-1757
- Kozanecki, A. & Groetzschel, R. (1990). Lattice location and optical activity of Yb in III-V semiconducting compounds, *Journal of Applied Physics*, Vol. 68, pp. 517-522
- Kranzer, D. (1974). Mobility of holes of zinc-blende III-V and II-VI compounds, *Physica status solidi (a)*, Vol. 26, No. 1, pp. 11-52, ISSN: 1521-396X
- Krukovsky, S.I., et al. (2004). Effect of rare earth addition on GaAs-based layers grown by liquid phase epitaxy, *The European Physical Journal: Applied Physics*, Vol. 27, pp. 177-79
- Kumar, A. & Bose, D.N. (1992). Liquid phase epitaxy growth of high purity InP using rare earth dysprosium gettering, *Materials Science and Engineering B*, Vol. 12, pp. 389-392

- Kumar, A.; Pal, D. & Bose, D. (1995). Liquid phase epitaxy growth of InGaAs with rare-earth gettering: characterization and deep level transient spectroscopy studies, *Journal of Electronic Materials*, Vol. 24, pp. 833-840
- Kuphal, E. (1981). Preparation and characterization of LPE InP, *Journal of Crystal Growth*, Vol. 54, pp. 117-126
- Kuphal, E. (1991). Liquid phase epitaxy, *Applied Physics A: Materials Science & Processing*, Vol. 52, No. 6, pp. 380-409
- Lee, C.T.; Yeh, J.H. & Lyu, Y.T. (1996). Characterization of Nd-doped AlGaAs grown by liquid phase epitaxy, *Journal of Crystal Growth*, Vol. 163, pp. 343-347
- Nakagome, H.; Takahei, K. & Homma, Y. (1987). Liquid phase epitaxy and characterization of rare-earth-ion (Yb, Er) doped InP, *Journal of Crystal Growth*, Vol. 85, pp. 345-356
- Nelson, H. (1963). Epitaxial growth from the liquid state and its application to the fabrication of tunnel and laser diodes, *RCA Review*, Vol. 24, pp. 603
- Nishikawa, H., et al. (1989). Etch Pit Observation of InP, *Japanese Journal of Applied Physics*, Vol. 28, No. 5, pp. 941-942
- Novák, J., et al. (1989). Growth and properties of low-doped InGaAs LPE layers using rare-earth oxides, *Journal of Crystal Growth*, Vol. 96, pp. 645-648
- Novák, J.; Hasenhorl, S. & Kuliffayová, M. (1991). Gettering properties of PrO<sub>2</sub> in In<sub>0.53</sub>Ga<sub>0.47</sub>As LPE growth, *Journal of Crystal Growth*, Vol. 110, pp. 862-866
- Novák, J.; Hasenhorl, S. & Malacký, L. (1993). Large activation of praseodymium in InGaAs, *Semiconductor Science and Technology*, Vol. 8, pp. 747-749
- Novotný, J., et al. (1999). Preparation and properties of Er and Yb doped InP-based semiconductor compounds, *Czechoslovak Journal of Physics*, Vol. 49, No. 5, pp. 757-763
- Pearsall, T.P., Ed. (2000). *Properties, Processing and Applications of Indium Phosphide*, INSPEC, The Institution of Electrical Engineers, London, UK, ISBN: 085296 949-x
- Pelfer, P.G. (2001). Present status and perspectives of the radiation detectors based on InP materials, *Nuclear Instruments and Methods in Physics Research A*, Vol. 458, pp. 400-5
- Procházková, O., et al. (1997). Effect of holmium addition during LPE growth on the properties of InP and GaInAsP layers, *Czechoslovak Journal of Physics*, Vol. 47, No. 7, pp. 685-691
- Procházková, O., et al. (1999). Effect of rare-earth addition on liquid phase epitaxial InP-based semiconductor layers, *Materials Science and Engineering*, Vol. B66, pp. 63-66
- Procházková, O. & Zavadil, J. (1999). Rare earth elements in semiconductors technology - Part I., *Science Foundation in China*, Vol. 7, No. 2, pp. 44-47, ISSN: 1005-0841
- Procházková, O., et al. (2002). Preparation of InP-based semiconductor materials with low density of defects: effect of Nd, Ho and Tb addition, *Materials Science and Engineering B*, Vol. 91-92, pp. 407-411
- Procházková, O., et al. (2005a). Preparation of p-type InP layers for detection of radiation, *Journal of Crystal Growth*, Vol. 275, No. 1-2, pp. e959-e963
- Procházková, O.; Zavadil, J. & Žďánský, K. (2005b). Effect of Fe inter-diffusion on properties of InP layers grown with addition of RE elements, *Physica Status Solidi C*, Vol. 4, pp. 1269-1274
- Procházková, O., et al. (2009). Impact of Pr on properties of InP based layers for light sources and detectors, *Physica Status Solidi (c)*, pp. In print

- Queisser, H.J. & Haller, E.E. (1988). Defects in Semiconductors: Some Fatal, Some Vital, *Science*, Vol. 281, No. 5379, pp. 945-950
- Rakovics, V., et al. (2002). Spectral characteristics of InGaAsP/InP infrared emitting diodes grown by LPE, *Materials Science and Engineering B*, Vol. 91-92, pp. 491-494
- Rhee, K. & Bhattacharya, K. (1983). Impurities and Traps in Liquid Phase Epitaxial InP in relation to melt prebaking, *Journal of Electrochemical Society: Solid State Science and Technology*, Vol. 130, pp. 700-703
- Simpson, J.R. (2001). Rare Earth Doped Fiber Fabrication: Techniques and Physical Properties, In *Rare Earth Doped Fiber Lasers and Amplifiers*. Digonnet, M.J.F. (Ed), 1, CRC, ISBN: 978-0824704582
- Skromme, B.J., et al. (1984). Identification of the residual acceptors in undoped high purity InP, *Applied Physics Letters*, Vol. 44, No. 3, pp. 319-321
- Swaminathan, V.; Donnelly, V.M. & Long, J. (1985). A photoluminescence study of Cd-related centers in InP, *Journal of Applied Physics*, Vol. 58, No. 12, pp. 4565-4572
- Takeda, Y., et al. (1976). Electron mobility and energy gap of In<sub>0.53</sub>Ga<sub>0.47</sub>As on InP substrate, Vol. 47, No. 12, pp. 5405-5408
- Thiel, C.W.; Sun, Y. & Cone, R.L. (2002). Progress in relating rare-earth ion 4f and 5d energy levels to host bands in optical materials for hole burning, quantum information and phosphors, *Journal of Modern Optics*, Vol. 49, pp. 2399-2411
- Wada, O. & Hasegawa, H., Eds. (1999). *InP-based Materials and Devices: Physics and Technology*, John Wiley & sons, ISBN: 0-471-18191-9
- Wu, M.C., et al. (1992). Erbium doping in InGaAsP grown by liquid phase epitaxy, *Journal of Applied Physics*, Vol. 71, pp. 456-460
- Wu, M.C. & Chiu, C. (1993). Very high purity InP layer grown by liquid-phase epitaxy using erbium gettering, *Journal of Applied Physics*, Vol. 73, pp. 468
- Zakharenkov, L.F., et al. (1981). *Fizika i Tekhnika Poluprovodnikov (Soviet Physics-Semiconductors)*, Vol. 15, pp. 1631-1636
- Zakharenkov, L.F., et al. (1997). Rare-Earth Elements in the Technology of III-V Compounds, In *Semiconductor Technology - Processing and Novel Fabrication Techniques*. Levinshtein, M.E. & Shur, M.S. (Eds), 91-130, John Wiley&Sons
- Zavada, J.M. & Zhang, D. (1995). Luminescence properties of erbium in III-V compound semiconductors, *Solid State Electronics*, Vol. 38, pp. 1285-1293
- Zavadil, J.; Procházková, O. & Žďánský, K. (1999). Rare Earth Elements in Semiconductors. Characterization -- part II. Proceedings of Proceedings of Advanced Materials and Devices for Optoelectronics, 48-51, Chinese Academy of Science, Beijing, China
- Zavadil, J., et al. (2007). Ce and Yb doped InP layers grown for radiation detection, *physica status solidi (c)*, Vol. 4, No. 4, pp. 1444-1447, ISSN: 1610-1642
- Žďánský, K.; Procházková, O. & Nohavica, D. (1999). Temperature dependence of electron Hall concentration in n-type InP and n-type InGaP. Proceedings of Proceedings of Advanced Materials and Devices for Optoelectronics, 25-43, Chinese Academy of Science, Beijing, China
- Žďánský, K., et al. (2001). P-type InP grown by LPE with rare earths: not intentional Ge acceptor doping, *Materials Science and Engineering B*, Vol. 80, pp. 10-13
- Žďánský, K., et al. (2002). P-type InP grown by liquid phase epitaxy from melts with rare earth admixtures, *Materials Science and Engineering B*, Vol. 91-92, pp. 38-42



## **Semiconductor Technologies**

Edited by Jan Grym

ISBN 978-953-307-080-3

Hard cover, 462 pages

**Publisher** InTech

**Published online** 01, April, 2010

**Published in print edition** April, 2010

Semiconductor technologies continue to evolve and amaze us. New materials, new structures, new manufacturing tools, and new advancements in modelling and simulation form a breeding ground for novel high performance electronic and photonic devices. This book covers all aspects of semiconductor technology concerning materials, technological processes, and devices, including their modelling, design, integration, and manufacturing.

### **How to reference**

In order to correctly reference this scholarly work, feel free to copy and paste the following:

Jan Grym, Olga Prochazkova, Jiri Zavadil and Karel Zdansky (2010). Role of Rare-Earth Elements in the Technology of III-V Semiconductors Prepared by Liquid Phase Epitaxy, Semiconductor Technologies, Jan Grym (Ed.), ISBN: 978-953-307-080-3, InTech, Available from:  
<http://www.intechopen.com/books/semiconductor-technologies/role-of-rare-earth-elements-in-the-technology-of-iii-v-semiconductors-prepared-by-liquid-phase-epita>

**INTECH**  
open science | open minds

### **InTech Europe**

University Campus STeP Ri  
Slavka Krautzeka 83/A  
51000 Rijeka, Croatia  
Phone: +385 (51) 770 447  
Fax: +385 (51) 686 166  
[www.intechopen.com](http://www.intechopen.com)

### **InTech China**

Unit 405, Office Block, Hotel Equatorial Shanghai  
No.65, Yan An Road (West), Shanghai, 200040, China  
中国上海市延安西路65号上海国际贵都大饭店办公楼405单元  
Phone: +86-21-62489820  
Fax: +86-21-62489821

© 2010 The Author(s). Licensee IntechOpen. This chapter is distributed under the terms of the [Creative Commons Attribution-NonCommercial-ShareAlike-3.0 License](#), which permits use, distribution and reproduction for non-commercial purposes, provided the original is properly cited and derivative works building on this content are distributed under the same license.

IntechOpen

IntechOpen